Passivity-based Formation Control for UAVs with a Suspended Load

Chris Meissen * **Kristian Klausen** ** **Murat Arcak** ***
Thor I. Fossen ** **Andrew Packard** *

* *Department of Mechanical Engineering at the University of California, Berkeley, CA, USA (cmeissen@berkeley.edu, apackard@berkeley.edu).*
** *Department of Engineering Cybernetics at the Norwegian University of Science and Technology, Trondheim, Norway (kristian.klausen@itk.ntnu.no, thor.fossen@ntnu.no).*
*** *Department of Electrical Engineering and Computer Sciences at the University of California, Berkeley, CA, USA (arcak@berkeley.edu).*

Abstract: This paper presents a passivity based formation control strategy for multiple unmanned aerial vehicles (UAVs) cooperatively carrying a suspended load. The control strategy we propose consists of an internal feedback control law for each UAV and a formation control law that regulates the relative position between each UAV. We show that under this control strategy the interconnected system has a continuum of equilibria and prove stability for all equilibrium points where the cables supporting the suspended load are in tension.

Keywords: Coordination of multiple vehicle systems, Passivity-based control, Control of interconnected systems, UAVs

1. INTRODUCTION

We consider multiple UAVs, specifically multicopters, transporting a suspended payload as in Figure 1. Many potential applications for this have been proposed, including package delivery and transportation, fire extinguishing, and geo-surveying and mine detection as in Bisgaard (2008); Mellinger et al. (2013).

Using multiple UAVs for this task is advantageous because it provides a higher load carrying capacity as well as having better control over the position and orientation of the suspended load. This is especially important in applications like geo-surveying where it is necessary to maintain the suspended load at a certain orientation relative to the ground. A multiple UAV configuration also reduces the effect of disturbances like wind on the motion of the suspended load. This is especially important for search and rescue or rendezvous operations as in Bernard et al. (2011) where precise position control is necessary.

Cooperative control of multiple UAVs carrying a suspended load has been studied under different scenarios. For example, Mellinger et al. (2013); Michael et al. (2011) assume external cameras are available to provide accurate position measurements of the UAVs and the payload, which limits the applicability of these approaches for large scale, outdoor environments. Alternatively, in Klausen et al. (2014); Maza et al. (2009); Bernard and Kondak (2009); Bernard et al. (2011) sensors onboard the UAVs are used to measure the relative positions of the UAVs and the payload, and use only these measurements to maintain a constant formation.

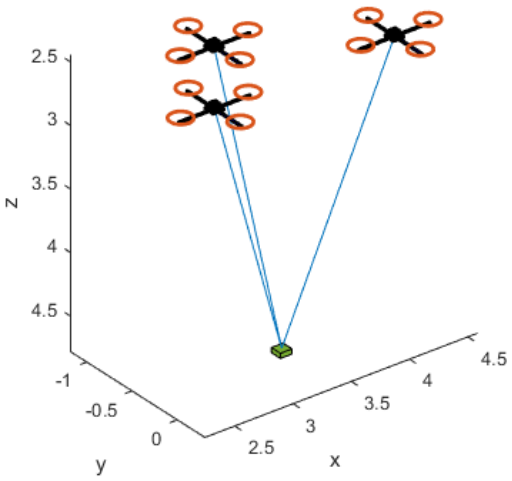

Fig. 1. Multiple UAVs carrying a suspended load.

In this paper we assume that the UAVs only measure their relative positions and not the position of the suspended load. We treat each UAV and the suspended load as individual subsystems and propose a passivity based formation control strategy similar to that in Arcak (2007); Bai et al. (2011) to stabilize the interconnected system. For each UAV we propose an internal control law rendering the system output strictly passive between the input, the force from the cables and formation control law, and the output, the velocity error. The formation control law can be interpreted as virtual springs between the UAVs, and the connection between the UAVs and the suspended load is modeled as a physical spring representing the cable. We

extend the framework in Bai et al. (2011) to allow for the suspended load and compensate for its effect on the UAVs.

First, we model the dynamics of the UAVs, suspended load, and cables between the UAVs and the load. Then, in Section 3 we propose an internal feedback control law for each UAV and a formation control law that regulates the relative position between each UAV. In Section 4 we show that the interconnected system has a continuum of equilibria and prove stability for all equilibrium points where the cables supporting the suspended load are in tension. Finally, we present simulation results using the proposed control strategy for a system with 3 UAVs.

1.1 Preliminaries

In order to prove stability of this system we decompose it into subsystems and characterize the input-output properties of each individual subsystem by showing they are equilibrium independent dissipative (EID) Hines et al. (2011); Bürger et al. (2014). Consider a system of the form

$$\dot{x}(t) = f(x(t), u(t)) \qquad y(t) = h(x(t), u(t)) \tag{1}$$

where there exists a nonempty set $\mathcal{X} \subseteq \mathbb{R}^n$ such that for each $\bar{x} \in \mathcal{X}$ there exists a unique $\bar{u} \in \mathbb{R}^m$ satisfying $f(\bar{x}, \bar{u}) = 0$.

Definition 1. The system (1) is *EID* on an open set $\mathcal{D} \subset \mathbb{R}^n$ with respect to a supply rate w if there exists a nonnegative storage function $V : \mathcal{D} \times \mathcal{D} \to \mathbb{R}_+$ such that $V(\bar{x}, \bar{x}) = 0$ and

$$\dot{V}(x, \bar{x}) \triangleq \nabla_x V(x, \bar{x})^\top f(x, u) \leq w(u - \bar{u}, y - \bar{y}) \tag{2}$$

for all $x \in \mathcal{D}$, $u \in \mathbb{R}^m$ and for all $\bar{x} \in \mathcal{D}$ and $\bar{u}$ that satisfy $f(\bar{x}, \bar{u}) = 0$ where $y = h(x, u)$ and $\bar{y} = h(\bar{x}, \bar{u})$.

This definition ensures dissipativity with respect to any possible equilibrium point rather than a particular point. This is advantageous for compositional analysis, since the equilibrium of an interconnected system may be hard to compute.

Furthermore, a system is *equilibrium independent passive* if it is EID with respect to the supply rate

$$w(u - \bar{u}, y - \bar{y}) = (u - \bar{u})^\top (y - \bar{y})$$

and it is *equilibrium independent output strictly passive* if it is EID with respect to the supply rate

$$w(u - \bar{u}, y - \bar{y}) = (u - \bar{u})^\top (y - \bar{y}) - \epsilon (y - \bar{y})^\top (y - \bar{y})$$

with $\epsilon > 0$.

2. SYSTEM DYNAMICS

We consider N UAVs that are cooperatively carrying a suspended load. The desired formation of the UAVs and the load in the $x-y$ plane are represented by an undirected graph as in Figure 2. We let $\eta_i \in \mathbb{R}^3$, $i = 1, \ldots, N$ and η_{N+1} be the position of the UAVs and the suspended load, respectively.

For each dotted edge $\ell = 1, \ldots, T$ in the graph between UAVs we assign one vertex to be the head if it is clockwise from the other vertex. Therefore, for the configuration in Figure 2 vertex 1 is the head and vertex 2 is the tail along edge 1. Solid edges $\ell = T + 1, \ldots, E$ represent the cable between the UAV and the load. We assign the UAV vertex

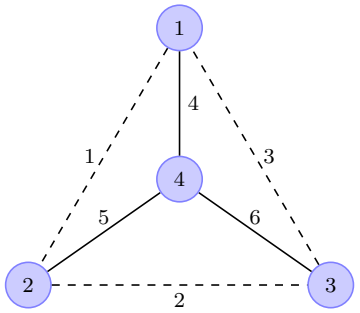

Fig. 2. Undirected graph of UAVs $(1, 2, 3)$ and the suspended load 4.

to be the head and the load vertex the tail. The incidence matrix, given by

$$M_{il} = \begin{cases} 1 & \text{if vertex } i \text{ is the head of edge } \ell \\ -1 & \text{if vertex } i \text{ is the tail of edge } \ell \\ 0 & \text{otherwise,} \end{cases} \tag{3}$$

will be used to characterize the interconnection topology.

Along each edge $\ell = 1, \ldots, E$ we define the relative position as $r_\ell(t) := \eta_i(t) - \eta_j(t) \in \mathbb{R}^3$ where i and j correspond to the head and tail vertices, respectively, of the ℓ-th edge.

Since the input and output of the UAVs and the suspended load is in three dimensions the matrix $D := M \otimes I_3$ maps the position of the UAVs to the relative positions $r_\ell(t) \in \mathbb{R}^3$ along each edge $\ell = 1, \ldots, E$ by

$$r = D^\top \eta. \tag{4}$$

As an example for the formation described in Figure 1 we have

$$M = \begin{bmatrix} 1 & 0 & -1 & 1 & 0 & 0 \\ -1 & 1 & 0 & 0 & 1 & 0 \\ 0 & -1 & 1 & 0 & 0 & 1 \\ 0 & 0 & 0 & -1 & -1 & -1 \end{bmatrix}$$

and

$$\begin{bmatrix} r_1 \\ r_2 \\ r_3 \\ r_4 \\ r_5 \\ r_6 \end{bmatrix} = D^\top \eta = \begin{bmatrix} \eta_1 - \eta_2 \\ \eta_2 - \eta_3 \\ \eta_3 - \eta_1 \\ \eta_1 - \eta_4 \\ \eta_2 - \eta_4 \\ \eta_3 - \eta_4 \end{bmatrix}.$$

The dynamics of each UAV are described by point mass models, as in Mahony et al. (2012); Klausen et al. (2014), of the form

$$m_i \dot{v}_i(t) = -m_i g + u_i^L(t) + \tau_i(t) \qquad i = 1, \ldots, N \tag{5}$$

with state $v_i(t) \in \mathbb{R}^3$, control input $\tau_i(t) \in \mathbb{R}^3$, mass m_i, and acceleration due to gravity $g \in \mathbb{R}^3$. The force applied to the UAV through the cable connected to the suspended load is $u_i^L(t) \in \mathbb{R}^3$. For each UAV an internal feedback controller will be used to compensate for this unknown force.

The dynamics of the suspended load are

$$m_L \dot{v}_{N+1}(t) = -m_L g + u_{N+1}(t) \tag{6}$$

with state $v_{N+1}(t) \in \mathbb{R}^3$, mass m_L, acceleration due to gravity g, and input $u_{N+1}(t) \in \mathbb{R}^3$ which is the sum of the forces applied to the load by the UAVs through the cables.

The edges $\ell = 1, \dots, T$ between UAVs do not represent a physical connection so in Section 3.2 a control law is proposed that acts as virtual springs oriented along the edges between the UAVs. The edges $\ell = T+1, \dots, E$ between the UAVs and the load represent a flexible cable. The force transferred along this cable is modeled by a function $h_\ell : \mathbb{R}^3 \to \mathbb{R}^3$ which takes the form

$$h_\ell(r_\ell) = \sigma_\ell(\|r_\ell\|)\frac{1}{\|r_\ell\|}r_\ell \tag{7}$$

where we assume $\sigma_\ell : \mathbb{R}_+ \to \mathbb{R}$ is strictly increasing and onto for $\ell = T+1, \dots, E$. This function can be interpreted as a spring acting between the UAV and the suspended load.

3. CONTROL STRATEGY

In this section, we describe an internal feedback control for each UAV that renders it EID and compensates for the vertical force applied to it by the suspended load. Then, a formation control strategy is presented that regulates the relative position of the UAVs in the x, y, and z coordinates independently.

3.1 Internal Feedback Control

We propose a passivity based design where the internal feedback for each UAV is

$$\tau_i(t) = m_i g + v^d - v_i(t) - \delta_i(t) + u_i^f(t) \tag{8}$$

where $m_i g$ compensates for the effect of gravity on the UAV, v^d is the desired velocity of the formation, and u_i^f is the formation control force which will regulate the relative positions of the UAVs as described in Section 3.2. The component $\delta_i(t)$ is updated by

$$\dot{\delta}_i(t) = v_i(t) - v^d \qquad \delta_i(0) = \hat{\delta}_i \tag{9}$$

where $\hat{\delta}_i$ is an estimate of the bias force applied to each UAV. The purpose of δ is to compensate for the vertical force applied to each UAV by the suspended load as well as compensate for other unmodeled bias forces like wind.

With this control strategy the UAV dynamics are

$$\begin{aligned} m_i\dot{v}_i(t) &= -v_i(t) + v^d - \delta_i(t) + u_i(t) \\ \dot{\delta}_i(t) &= v_i(t) - v^d \end{aligned} \tag{10}$$

where $u_i = u_i^f + u_i^L$ is the sum of the formation control force u_i^f and the force from the suspended load u_i^L. In Section 4 we show that this choice of τ guarantees that the system (10) is equilibrium independent output strictly passive from the input u_i to the output v_i.

3.2 Formation Control

The interconnected system can be represented as the block diagram in Figure 3. The Σ_i subsystems mapping u_i to v_i are the UAV ($i = 1, \dots, N$) and suspended load ($i = N+1$) subsystems and the Λ_ℓ subsystems mapping w_ℓ to $y_\ell = h(r_\ell)$ for $\ell = 1, \dots, E$ are the edge subsystems.

As depicted in Figure 3 we express the edge subsystems as

$$\begin{aligned} \dot{r}_\ell &= w_\ell \\ y_\ell &= h_\ell(r_\ell) \end{aligned} \tag{11}$$

where $w \triangleq D^\top v$ is the input to the edge subsystems and y is the output. For the edges $\ell = 1, \dots, T$ the functions h_ℓ

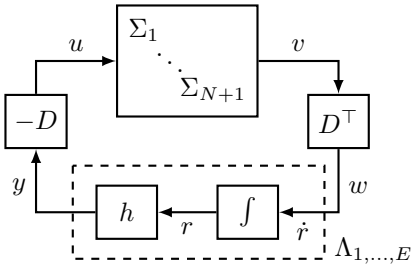

Fig. 3. Block diagram of the vehicle platoon dynamics.

characterize the formation control strategy, while for the edges $\ell = T+1, \dots, E$ they model the cable connecting the UAVs and the suspended load.

The formation control strategy, which requires measurement of the relative positions of the UAVs, is described by the functions $h_\ell : \mathbb{R}^3 \to \mathbb{R}^3$ of the form

$$h_\ell(r_\ell) = \begin{bmatrix} \sigma_\ell^x(r_\ell^x) \\ \sigma_\ell^y(r_\ell^y) \\ \sigma_\ell^z(r_\ell^z) \end{bmatrix} \tag{12}$$

for each edge $\ell = 1, \dots, T$ between UAVs. Similarly to (7) we assume that $\sigma_\ell^x, \sigma_\ell^y, \sigma_\ell^z : \mathbb{R} \to \mathbb{R}$ are strictly increasing and onto for $\ell = 1, \dots, T$. This control law can be interpreted as three virtual springs for each edge connecting UAVs that act independently in each coordinate.

The input to the UAVs is then

$$u = -D \begin{bmatrix} h_1(r_1) \\ \vdots \\ h_E(r_E) \end{bmatrix} \tag{13}$$

where h_ℓ are given by (12) for $\ell = 1, \dots, T$ and by (7) for $\ell = T+1, \dots, E$. Therefore, the input applied to the i-th subsystem is

$$u_i = -\sum_{\ell=1}^{E} D_{il} h_\ell(r_\ell) \tag{14}$$

which depends only on locally available measurements because $D_{il} \neq 0$ only when vertex i is the head or tail of edge ℓ.

4. STABILITY ANALYSIS

We analyze the stability properties of the system and proposed control laws using a compositional approach. Specifically, for each subsystem (i.e. UAV, load, or edge) we find a storage function certifying that it is EID. From these storage functions we then obtain a Lyapunov function for the interconnected system.

For each UAV $i = 1, \dots N$, described by (10), the storage function

$$S_i(v_i, \bar{v}_i, \delta_i, \bar{\delta}_i) = \frac{m_i}{2}\|v_i - \bar{v}_i\|^2 + \frac{1}{2}\|\delta_i - \bar{\delta}_i\|^2 \tag{15}$$

certifies equilibrium independent output strict passivity since

$$\begin{aligned} &\dot{S}_i(v_i, \bar{v}_i, \delta_i, \bar{\delta}_i) \\ &\quad = (v_i - \bar{v}_i)^\top(-v_i + v^d - \delta_i + u_i) + (\delta_i - \bar{\delta}_i)^\top(v_i - v^d) \\ &\quad = -\|v_i - \bar{v}_i\|^2 + (v_i - \bar{v}_i)^\top(u_i - \bar{u}_i) \end{aligned}$$

where we have used $\bar{v}_i = v^d$ and $\bar{u}_i = \bar{\delta}_i$ in the second equality.

For the suspended load, described by (6), the storage function

$$S_L(v_{N+1}, \bar{v}_{N+1}) = \frac{m_L}{2}\|v_{N+1} - \bar{v}_{N+1}\|^2 \tag{16}$$

can be used to show that it is equilibrium independent passive since

$$\begin{aligned}\dot{S}_L(v_{N+1}, \bar{v}_{N+1}) &= (v_{N+1} - \bar{v}_{N+1})^\top(-m_L g + u_{N+1}) \\ &= (v_{N+1} - \bar{v}_{N+1})^\top(u_{N+1} - \bar{u}_{N+1})\end{aligned}$$

where $\bar{u}_{N+1} = m_L g$.

For each edge $\ell = 1, \ldots, T$, described by (11) with the control strategy in (12), the storage function is

$$\begin{aligned}R_\ell(r_\ell, \bar{r}_\ell) &= \int_{\bar{r}_\ell}^{r_\ell} (h_\ell(\zeta) - h_\ell(\bar{r}_\ell))d\zeta \\ &= \sum_{i\in\{x,y,z\}} \int_{\bar{r}_\ell^i}^{r_\ell^i} (\sigma_\ell^i(\zeta^i) - \sigma_\ell^i(\bar{r}_\ell^i))d\zeta^i\end{aligned} \tag{17}$$

where the second equality holds since the curl of h_ℓ in (12) is zero implying path independence of the integral. The storage function R_ℓ is zero for $r_\ell = \bar{r}_\ell$ and strictly positive for all $r_\ell \neq \bar{r}_\ell$ since σ_ℓ^x, σ_ℓ^y, and σ_ℓ^z are strictly increasing and onto for $\ell = 1, \ldots, T$. This storage function certifies each subsystem is equilibrium independent passive since

$$\begin{aligned}\dot{R}_\ell(r_\ell, \bar{r}_\ell) &= \begin{bmatrix}\sigma_\ell^x(r_\ell^x) - \sigma_\ell^x(\bar{r}_\ell^x) \\ \sigma_\ell^y(r_\ell^y) - \sigma_\ell^y(\bar{r}_\ell^y) \\ \sigma_\ell^x(r_\ell^z) - \sigma_\ell^z(\bar{r}_\ell^z)\end{bmatrix}^\top w_\ell \\ &= (h_\ell(r_\ell) - h_\ell(\bar{r}_\ell))^\top(w_\ell - \bar{w}_\ell)\end{aligned}$$

where $\bar{w}_\ell = 0$.

For each edge $\ell = T+1, \ldots, E$, described by (11) and (7), the storage function is

$$R_\ell(r_\ell, \bar{r}_\ell) = \int_{\|\bar{r}_\ell\|}^{\|r_\ell\|} \sigma_\ell(\zeta)d\zeta - \sigma_\ell(\|\bar{r}\|)\frac{\bar{r}_\ell^\top(r_\ell - \bar{r}_\ell)}{\|\bar{r}_\ell\|}. \tag{18}$$

Clearly, $R_\ell(\bar{r}_\ell, \bar{r}_\ell) = 0$ and by calculating the Hessian of R_ℓ we can show that it is positive definite in a neighborhood of $\bar{r}_\ell$.

The gradient of the storage function is

$$\begin{aligned}\nabla_{r_\ell} R_\ell(r_\ell, \bar{r}_\ell) &= \sigma_\ell(\|r_\ell\|)\frac{r_\ell}{\|r_\ell\|} - \sigma_\ell(\|\bar{r}_\ell\|)\frac{\bar{r}_\ell}{\|\bar{r}_\ell\|} \\ &= h_\ell(r_\ell) - h_\ell(\bar{r}_\ell)\end{aligned}$$

and the Hessian is

$$\begin{aligned}&H_{r_\ell} R_\ell(r_\ell, \bar{r}_\ell) \\ &\quad= \nabla_{r_\ell}\left(\sigma_\ell(\|r_\ell\|)\frac{r_\ell^\top}{\|r_\ell\|}\right) \\ &\quad= \frac{\sigma_\ell(\|r_\ell\|)}{\|r_\ell\|} I_3 + \nabla_{r_\ell}\left(\frac{\sigma_\ell(\|r_\ell\|)}{\|r_\ell\|}\right) r_\ell^\top \\ &\quad= \frac{\sigma_\ell(\|r_\ell\|)}{\|r_\ell\|} I_3 + \left(\sigma_\ell'(\|r_\ell\|) - \frac{\sigma_\ell(\|r_\ell\|)}{\|r_\ell\|}\right)\frac{1}{r_\ell^\top r_\ell} r_\ell r_\ell^\top\end{aligned}$$

where $I_n \in \mathbb{R}^{n\times n}$ is the identity matrix. Note that the Hessian is the sum of a scaled identity matrix and a rank one matrix. Therefore, the eigenvalues of the Hessian are

$$\frac{\sigma_\ell(\|r_\ell\|)}{\|r_\ell\|}$$

with multiplicity 2 and

$$\frac{\sigma_\ell(\|r_\ell\|)}{\|r_\ell\|} + \left(\sigma_\ell'(\|r_\ell\|) - \frac{\sigma_\ell(\|r_\ell\|)}{\|r_\ell\|}\right) = \sigma_\ell'(\|r_\ell\|)$$

with multiplicity 1. Thus, if

$$\sigma_\ell(\|\bar{r}_\ell\|) > 0 \quad \text{and} \quad \sigma_\ell'(\|\bar{r}_\ell\|) > 0 \tag{19}$$

then the Hessian is positive definite at $\bar{r}_\ell$ which implies that $R_\ell(r_\ell, \bar{r}_\ell) > 0$ for all $r_\ell \neq \bar{r}_\ell$ in a neighborhood of $\bar{r}_\ell$. The first condition, $\sigma_\ell(\|\bar{r}_\ell\|) > 0$, holds whenever the spring is in tension and the second condition, $\sigma_\ell'(\|\bar{r}_\ell\|) > 0$, always holds since σ_ℓ is increasing.

The Lie derivative of this storage function is

$$\dot{R}_\ell(r_\ell, \bar{r}_\ell) = (h_\ell(r_\ell) - h_\ell(\bar{r}_\ell))^\top(w_\ell - \bar{w}_\ell)$$

where $\bar{w}_\ell = 0$. Therefore, this storage function certifies the edge subsystems are equilibrium independent passive in a neighborhood of $\bar{r}_\ell$ for any $\bar{r}_\ell$ satisfying $\sigma_\ell(\|\bar{r}_\ell\|) > 0$.

In order to characterize the equilibrium points of the system we must consider configurations with specific numbers of UAVs. For example with N = 2, the set of equilibria of the interconnected system in Figure 3 with the UAV, edge, and load subsystems described by (10), (11), and (6) respectively, is given by

$$\mathcal{E} = \left\{ (\bar{v}, \bar{\delta}, \bar{r}) \;\middle|\; \begin{array}{r} \bar{v}_i = v^d \text{ for } i = 1, \ldots, 3 \\ m_L g = h_2(\bar{r}_2) + h_3(\bar{r}_3) \\ \bar{\delta} = \begin{bmatrix} -h_1(\bar{r}_2 - \bar{r}_3) - h_2(\bar{r}_2) \\ h_1(\bar{r}_2 - \bar{r}_3) - h_3(\bar{r}_3) \end{bmatrix} \end{array} \right\}.$$

where the geometric relation $\bar{r}_1 = \bar{r}_2 - \bar{r}_3$ is used in the last equation. Since the functions $h_1, \ldots, h_3$ are increasing and onto in each coordinate there exists a unique $\bar{\delta}$ for all values of $\bar{r}_2$ and $\bar{r}_3$. Therefore, there is an equilibrium point for any r_2 and r_3 satisfying $m_L g = h_2(r_2) + h_3(r_3)$. For configurations with $N > 2$ UAVs the set of equilibria $\mathcal{E}$ is of a similar form and is a continuum of points.

Theorem 2. Any equilibrium point $(\bar{v}, \bar{\delta}, \bar{r}) \in \mathcal{E}$ of the interconnected system in Figure 3 that satisfies $\sigma_\ell(\|\bar{r}_\ell\|) > 0$ for $\ell = T+1, \ldots, E$ is stable.

Proof: By combining the subsystem storage functions (15)-(18) we get the candidate Lyapunov function

$$\begin{aligned}V(v, \delta, r) = &\sum_{i=1}^{N} S_i(v_i, \bar{v}_i, \delta_i, \bar{\delta}_i) \\ &+ S_L(v_{N+1}, \bar{v}_{N+1}) + \sum_{\ell=1}^{E} R_\ell(r_\ell, \bar{r}_\ell).\end{aligned} \tag{20}$$

for any equilibrium point $(\bar{v}, \bar{\delta}, \bar{r}) \in \mathcal{E}$. By the definitions of the subsystem storage functions $V(\bar{v}, \bar{\delta}, \bar{r}) = 0$ and V is positive definite in v, δ, and r_ℓ for $\ell = 1, \ldots, T$. Furthermore, since $\sigma_\ell(\|\bar{r}_\ell\|) > 0$ for $\ell = T+1, \ldots, E$ then there will exist an open set $\mathcal{R}$ containing $\bar{r}_\ell$ such that $V(\bar{v}, \bar{\delta}, \bar{r}) = 0$ and $V(\bar{v}, \bar{\delta}, r) > 0$ for any $\{r_\ell \in \mathcal{R} \mid r_\ell \neq \bar{r}_\ell \text{ for } \ell = T+1, \ldots, 1\}$.

The Lie derivative of V is

$$
\begin{aligned}
&\dot{V}(v,\delta,r) \\
&\quad = \sum_{i=1}^{N} \left(-\|v_i - \bar{v}_i\|^2 + (v_i - \bar{v}_i)^\top (u_i - \bar{u}_i) \right) \\
&\qquad + (v_{N+1} - \bar{v}_{N+1})^\top (u_{N+1} - \bar{u}_{N+1}) \\
&\qquad + \sum_{\ell=1}^{E} (h_\ell(r_\ell) - h_\ell(\bar{r}_\ell))^\top (w_\ell - \bar{w}_\ell) \\
&\quad = -\sum_{i=1}^{N} \|v_i - \bar{v}_i\|^2 + (v - \bar{v})^\top (u - \bar{u}) \\
&\qquad + (h(r) - h(\bar{r}))^\top (w - \bar{w}) \\
&\quad = -\sum_{i=1}^{N} \|v_i - \bar{v}_i\|^2 - (v - \bar{v})^\top D(h(r) - h(\bar{r})) \\
&\qquad + (v - \bar{v})^\top D(h(r) - h(\bar{r})) \\
&\quad = -\sum_{i=1}^{N} \|v_i - \bar{v}_i\|^2 \leq 0
\end{aligned}
$$

where the third inequality follows from $u = -Dh(r)$ and $w = D^\top v$. Hence, any equilibrium point $(\bar{v}, \bar{\delta}, \bar{r})$ satisfying $\sigma_\ell(\|\bar{r}_\ell\|) > 0$ for $\ell = T+1, \ldots, E$ is stable. ■

Remark 3. The assumption that $\sigma_\ell(\|\bar{r}_\ell\|) > 0$ for $\ell = T+1, \ldots, E$ is not restrictive because it is only true when the cables between the UAVs and the load are in tension. This condition is expected in normal operation and desired so that there is no slack in the cables.

5. APPLICATION EXAMPLE

As an example, consider the configuration in Figure 2 with $N = 3$ UAVs carrying the suspended load. Let each UAV have a mass $m = 2$ kg, and the load have mass $m_L = 3$ kg. In addition to the reaction force from the load, the UAVs are also affected by a constant wind in the x-direction with a magnitude of 4 m/s.

For $N = 3$, a fully connected graph between all UAVs consists of three links and the resulting control incidence matrix M_c is given by

$$
M_c = \begin{bmatrix} 1 & 0 & -1 \\ -1 & 1 & 0 \\ 0 & -1 & 1 \end{bmatrix} \tag{21}
$$

Suppose we want the three UAVs to form a triangle with each side having length $\Delta \in \mathbb{R}$. We let $\eta_i^d \in \mathbb{R}^3$ for $i = 1, \ldots, N$ represent the desired positions of the UAVs and assume that

$$
\eta_1^d = \begin{bmatrix} 0 \\ 0 \\ 0 \end{bmatrix}.
$$

Then a set of possible desired positions of the UAVs are described by

$$
\eta_2^d = \begin{bmatrix} \Delta \\ 0 \\ 0 \end{bmatrix} \quad \text{and} \quad \eta_3^d = \begin{bmatrix} \Delta/2 \\ \sqrt{\Delta^2 - \Delta^2/2^2} \\ 0 \end{bmatrix}.
$$

The desired relative positions $r_\ell^d \in \mathbb{R}^3$ are then given by

$$
\begin{bmatrix} r_1^d \\ r_2^d \\ r_3^d \end{bmatrix} = (M_c \otimes I_3)^\top \begin{bmatrix} \eta_1^d \\ \eta_2^d \\ \eta_3^d \end{bmatrix}. \tag{22}
$$

We then design h_ℓ as described in Section 3.2. Specifically, we choose the formation control feedback function h_ℓ for $\ell = 1, \ldots, T$ to be

$$
h_\ell(r_\ell) = k(r_\ell - r_\ell^d) \tag{23}
$$

with $k = 8$. Since k is positive h_ℓ is strictly increasing and onto.

Note that without the suspended load the relative positions r_ℓ of the UAVs would converge to the desired relative positions r_ℓ^d. However, the force from the suspended load will pull the UAVs slightly closer together, so the equilibrium $\bar{r}_\ell$ for the links between the UAVs will be slightly different from r_ℓ^d.

The force between the load and the UAVs are modeled by Hooke's law as

$$
\sigma_\ell(\|r_\ell\|) = \gamma(\|r_\ell\| - L_\ell) \tag{24}
$$

for $\ell = T+1, \ldots, E$, where $L_\ell = 2$ is the nominal length of the wire at link ℓ. The wires are modeled as relatively stiff springs with $\gamma = 100$.

6. RESULTS

We let the initial positions of the UAVs be

$$
\eta_1^0 = \begin{bmatrix} 0 \\ 0 \\ 0 \end{bmatrix}, \quad \eta_2^0 = \begin{bmatrix} 3 \\ 0 \\ 0 \end{bmatrix}, \quad \eta_3^0 = \begin{bmatrix} 0 \\ 1 \\ 0 \end{bmatrix},
$$

the desired formation be given by (22) with $\Delta = 2$, and the desired velocity be $v^d = [0\ 0\ 0]^\top$. The results of the simulation can be seen in Figures 4–7. The relative movements of the three UAVs can be seen in Figure 4, where the star represents the initial position, and the UAV drawing is the final position. As can be seen, they approach the desired relative formation, and the velocity error $|v_i(t) - v^d(t)|$ converges to zero in Figure 5. From Figure 6 we see that the distance between the UAVs converge to a constant value, but as expected, it is slightly less than Δ.

Figure 7 shows estimates of the load mass and wind bias, which converge to the true values. The estimated load mass is calculated by summing the z-components of δ_i, while the estimated wind bias is the average of the xy-components.

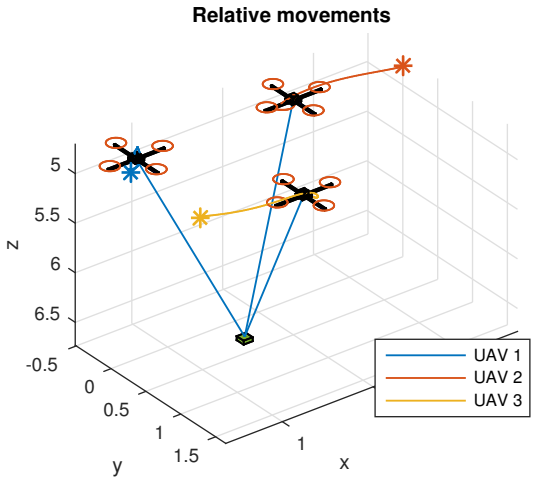

Fig. 4. Position of the three UAVs and the suspended load.

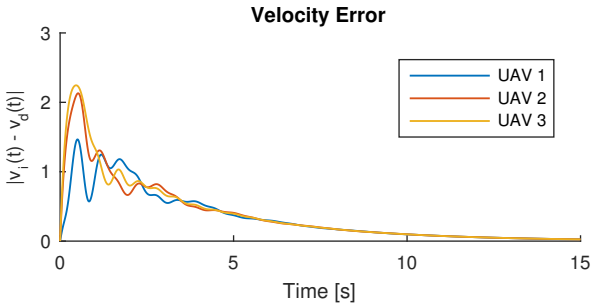

Fig. 5. The velocity error relative to the desired velocity v^d for each UAV.

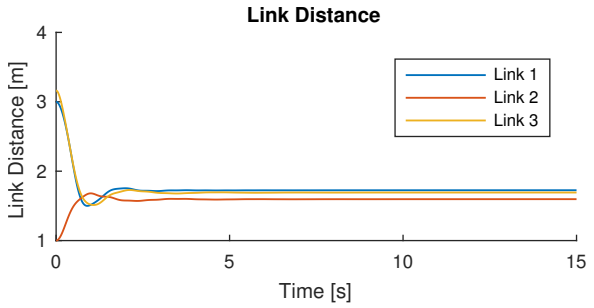

Fig. 6. Distance between each UAV.

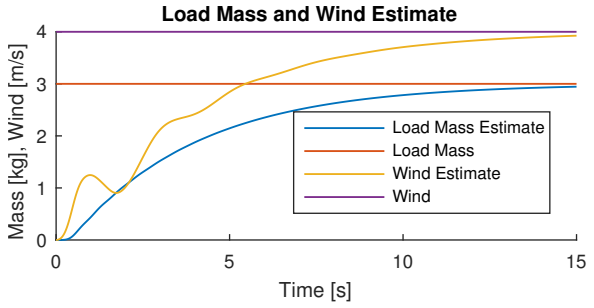

Fig. 7. Load and bias estimates, as calculated from the integral terms δ_i of each UAV.

7. CONCLUSION

In this paper, passivity-based control design was applied to a system of multiple UAVs carrying a suspended load. The proposed control strategy regulates the relative position between the UAVs and compensates for the vertical force applied by the suspended load. We prove that the equilibrium points of the system when the cables are in tension are stable and provide simulation results demonstrating the performance of the control strategy.

REFERENCES

Arcak, M. (2007). Passivity as a design tool for group coordination. *IEEE Transactions on Automatic Control*, 52(8), 1380–1390. doi:10.1109/TAC.2007.902733.

Bai, H., Arcak, M., and Wen, J. (2011). *Cooperative Control Design: A Systematic, Passivity-Based Approach.* Communications and Control Eng. Springer, New York.

Bernard, M. and Kondak, K. (2009). Generic slung load transportation system using small size helicopters. *2009 IEEE International Conference on Robotics and Automation*, 3258–3264.

Bernard, M., Kondak, K., Maza, I., and Ollero, A. (2011). Autonomous transportation and deployment with aerial robots for search and rescue missions. *Journal of Field Robotics*, 28(6), 914–931.

Bisgaard, M. (2008). *Modeling, Estimation, and Control of Helicopter Slung Load System.* Ph.D. thesis, Aalborg University.

Bürger, M., Zelazo, D., and Allgöwer, F. (2014). Duality and network theory in passivity-based cooperative control. *Automatica*, 50(8), 2051–2061.

Hines, G., Arcak, M., and Packard, A. (2011). Equilibrium-independent passivity: a new definition and numerical certification. In *Automatica*, 1949–1956.

Klausen, K., Fossen, T.I., and Johansen, T.A. (2014). Suspended load motion control using multicopters. In *Mediterranean Conference on Control and Automation.*

Mahony, R., Kumar, V., and Corke, P. (2012). Multirotor aerial vehicles: Modeling, estimation, and control of quadrotor. *IEEE Robotics Automation Magazine*, 19(3), 20–32. doi:10.1109/MRA.2012.2206474.

Maza, I., Kondak, K., Bernard, M., and Ollero, A. (2009). Multi-uav cooperation and control for load transportation and deployment. *Journal of Intelligent and Robotic Systems*, 57(1), 417–449.

Mellinger, D., Shomin, M., Michael, N., and Kumar, V. (2013). *Cooperative grasping and transport using multiple quadrotors*, 545–558. Springer Berlin Heidelberg.

Michael, N., Fink, J., and Kumar, V. (2011). Cooperative manipulation and transportation with aerial robots. *Autonomous Robots*, 30(1), 73–86.